CHAPTER IV
RESULTS AND DISCUSSION

4.1 Equilibration Time Determination

Mercury concentration was investigated for its equilibration time. Methylcyclohexane and toluene representing cyclic aliphatic and aromatic hydrocarbons, respectively were chosen in this experiment. To observe the equilibration time, the solvent with mercury droplet was shaken at the controlled speed of 55 rpm and the temperature of 5±0.01°C for total 35-45 hours and the results are presented in Figures 4.1-4.2.

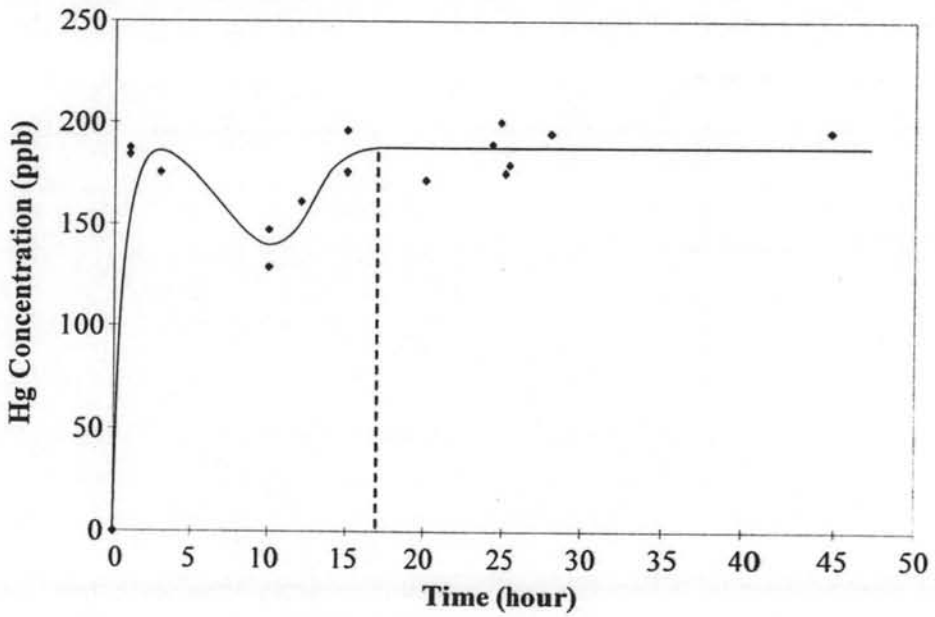

Figure 4.1 Mercury concentration of methylcyclohexane as a function of time at 5°C.

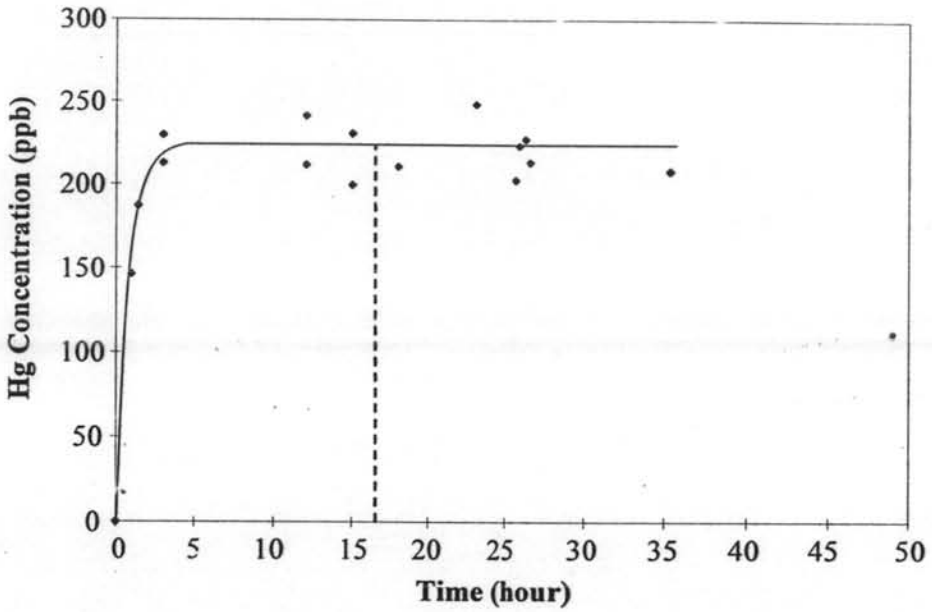

Figure 4.2 Mercury concentration of toluene as a function of time at 5°C.

Figure 4.1 shows that mercury concentration in methylcyclohexane increased considerably at the first few hours, slightly decreased within 10 hours and then increased again and remained constant around 180 ppb after 17 hours. The declined solubility around the fifth hour was possibly due to inequilibrium adsorption of mercury on the glass wall. Mercury concentration in toluene considerably increased and remained stable about 220 ppb after 5 hours. It was observed that the selected solvents have constant mercury concentrations after shaking for 17 hours. Generally, the kinetic equilibrium at high temperature is faster than that at low temperature. Therefore, at least 17 hours equilibrium time was required to guarantee equilibrium condition. As the kinetics of solvation depends on the temperature, agitation and surface area of solute, these affecting parameters were well controlled as well as the drop size of mercury.

4.2 Mercury Solubility Study

4.2.1 Solubility of Mercury in Single Solvents

4.2.1.1 Effect of Mercury in Headspace and Suspended Mercury

The experiment was carefully performed to check for possible factors that could affect the solubility of mercury and accuracy, *i.e.* the mercury in headspace and suspended mercury during shaking periods. To observe the mercury content in headspace, cyclohexane at the highest studied temperature (40°C) was selected because its vapor pressure is the highest. The results of mercury solubility at 40°C are tabulated in Table 4.1. Only two percent of mercury in the liquid was transferred to the vapor phase.

Table 4.1 Mercury content in vapor and liquid phases in cyclohexane at 40°C

Solvent	Test no.	Mercury concentration (µg/L)		Vapor-liquid distribution of mercury content
		Vapor phase	Liquid phase	
Cyclohexane	1	40	1896	2.09
	2	35	1800	1.96
	3	36	1908	1.88
	Mean	*37±2*	*1868±59*	*1.98±0.1*

For suspended mercury, the filtration test was performed with solubility of mercury in *n*-heptane at 25°C with and without filtration. The solvent (2 ml) was introduced to a plastic disposal filter (0.22 micron). The operating temperature of 25°C was selected to avoid the error from temperature variation during filtration. The concentration deviation obtained from with and without filtration was 4.54%. However, it was considered within the operating error range (Rochana, 2006). It was important to note that any suspended mercury occurred under this experimental condition was within an acceptable error and had less effect to the mercury solubility in liquid hydrocarbon.

4.2.1.2 Mercury Solubility

The results of mercury solubility are shown in Figure 4.3. Cyclohexane showed the highest mercury solubility, and the others were comparable at low temperature (15°C) but significantly different at high temperature. For all hydrocarbons, the solubility was varied from 180 to 2500 ppb depending on types of hydrocarbons. The solubility of mercury in cyclohexane at 5 °C could not be determined because it is below the melting point (6.5°C). The mercury solubility in ethylbenzene showed abnormal solubility which will be discussed separately.

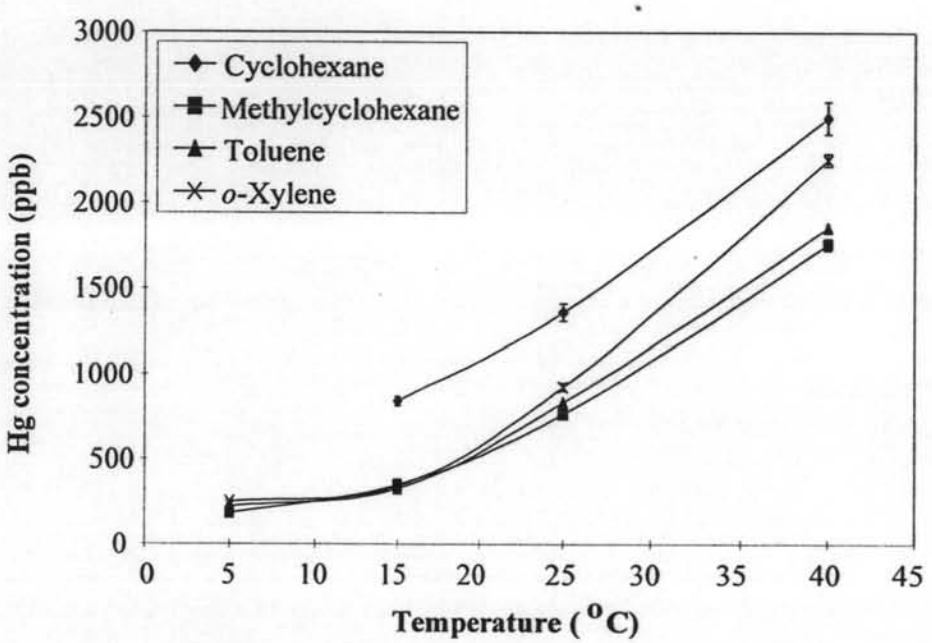

Figure 4.3 Temperature dependence of mercury solubility in hydrocarbons at the temperature range of 5-40°C.

Figures 4.4-4.7 demonstrate the exponential plots in logarithmic scale where X is mole fraction and T is absolute temperature in Kelvin. The curves were fitted well with a linear relation and their coefficients are presented in Table 4.2. It was found that the solubility curves of all hydrocarbons were linear with R^2 better than 0.97. The results confirmed that the mercury solubility in hydrocarbons showed exponential increase with temperature. Comparisons of this work with literature values are presented in Tables 4.3-4.6. The values from this work were

much lower than the reported values. The difference between this work and the other work can be interpreted based on several reasons. Firstly, the experimental condition was different, *i.e.* shaking time, speed and mode of shaking device and pretreatment step. Secondly the analytical equipment and techniques were also different. However, results from this work were similar to results from other work (Spencer and Voigt, 1968) in that the solubility curves were exponential function of temperature.

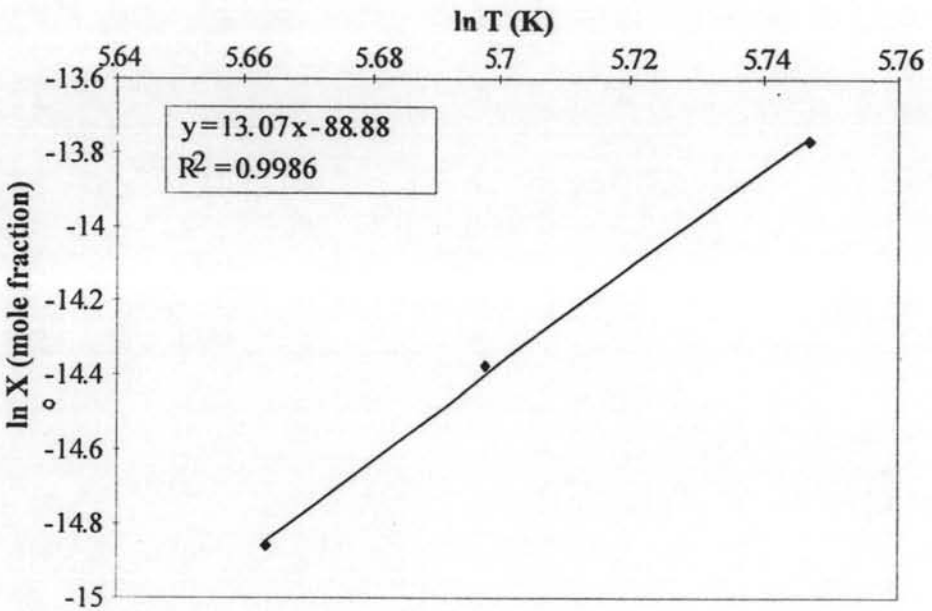

Figure 4.4 Temperature dependence of mercury solubility in cyclohexane at the temperature range of 5-40°C.

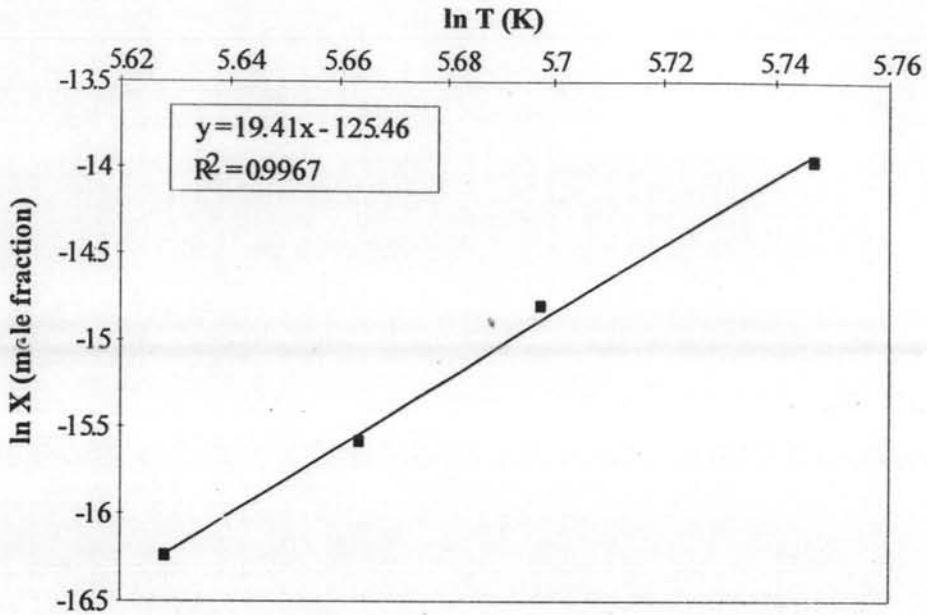

Figure 4.5 Temperature dependence of mercury solubility in methylcyclohexane at the temperature range of 5-40°C.

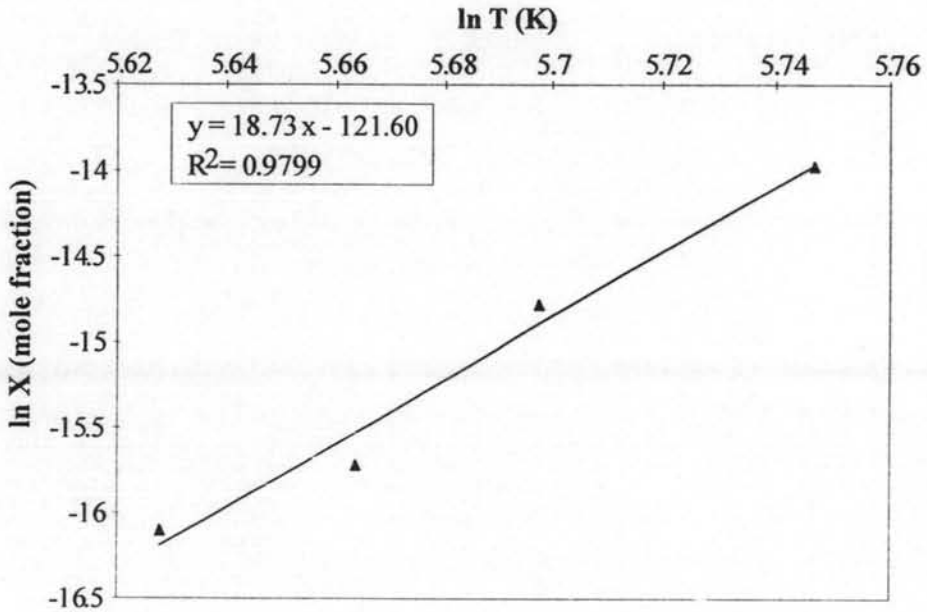

Figure 4.6 Temperature dependence of mercury solubility in toluene at the temperature range of 5-40°C.

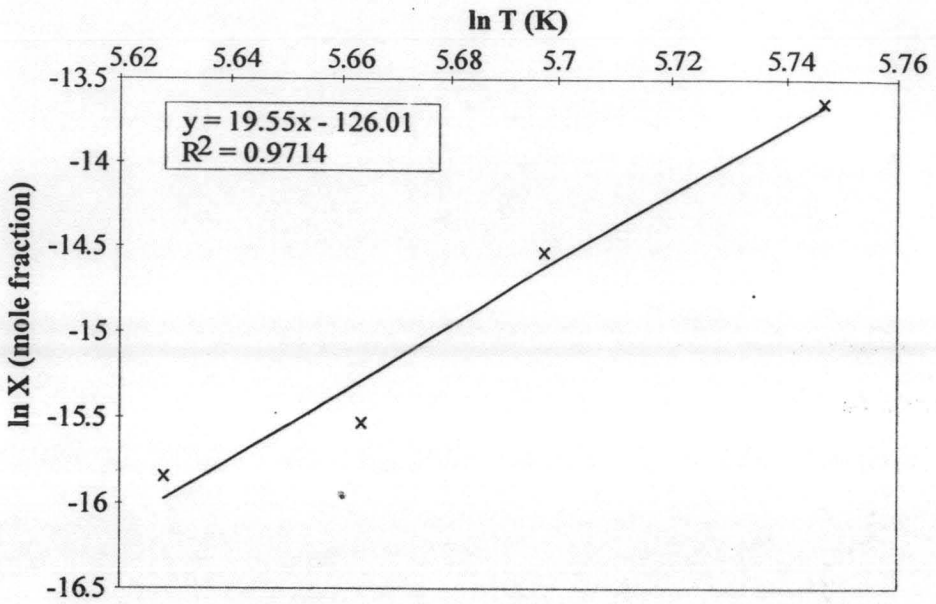

Figure 4.7 Temperature dependence of mercury solubility in *o*-xylene at the temperature range of 5-40°C.

Table 4.2 The coefficients of least-squares equation of lnX=AlnT+B at the temperature range of 5-40°C

Solvent	A	B
Cyclohexane	13.07	88.89
Methylcyclohexane	19.41	125.46
Toluene	18.73	121.60
o-Xylene	19.55	126.01

Table 4.3 Mercury solubility in hydrocarbons at 5°C

Solvent	Mercury concentration (ppb)		
	Literature values (Spencer and Voigt, 1968)*	This work	% Difference **
Cyclohexane	-	-	-
Methylcyclohexane	763	181 ± 7	76
Toluene	917	222 ± 7	76
o-Xylene	809	247 ± 7	69
Ethylbenzene	-	>17575	-

* Obtained from their empirical equation

** Compared between Spencer et al's result and experimental result

Table 4.4 Mercury solubility in hydrocarbons at 15°C

Solvent	Mercury concentration (ppb)		
	Literature values (Spencer and Voigt, 1968)*	This work	% Difference **
Cyclohexane	1957	839 ± 28	112
Methylcyclohexane	1343	349 ± 1	74
Toluene	1616	326 ± 13	80
o-Xylene	1509	340 ± 11	77
Ethylbenzene	-	-	-

* Obtained from their empirical equation

** Compared between Spencer and Voigt's result and experimental result

Table 4.5 Mercury solubility in hydrocarbons at 25°C

Solvent	Mercury concentration (ppb)			
	Literature values (Spencer and Voigt, 1968)*	Literature values (Kuntz and Main, 1964)**	This work	% Difference ***
Cyclohexane	3112 ± 77	2829	1360 ± 51	56
Methylcyclohexane	2400 ± 9	-	763 ± 18	67
Toluene	2780 ± 23	2895	830 ± 5	70
o-Xylene	2732 ± 68	-	922 ± 24	66
Ethylbenzene	-	-	-	-

* Radiotracer technique as analytical method in µmole/L converted to ppb

** Reported from a previous work in µmole/L converted to ppb

*** Compared between Spencer and Voigt's result and experimental result

Table 4.6 Mercury solubility in hydrocarbons at 40°C

Solvent	Mercury concentration (ppb)		
	Literature values (Spencer and Voigt, 1968)*	This work	% Difference **
Cyclohexane	5840	2500 ± 96	57
Methylcyclohexane	5090	1756 ± 37	65
Toluene	6134	1855 ±22	70
o-Xylene	6542	2252 ± 38	66
Ethylbenzene	-	-	-

* Obtained from their empirical equation

** Compared between Spencer and Voigt's result and experimental result

It is very interesting to compare the solubility data using solubility parameter (Barton, 1991) and regular solution (Hildebrand *et al.*, 1962). Thermodynamics was applied to explain the solubility of mercury in hydrocarbons. The theories predict solubility as a function of temperature and solubility parameter. Hildebrand–Scatchard equation ($-RT\ln {}^{j}x_s = {}^{j}V({}^{j}\delta - {}^{l}\delta)^2$) and Hansen parameter ($\delta_t^2 = \delta_d^2 + \delta_p^2 + \delta_h^2$) were described. The solubility parameter is the most important factor and can be used to describe the solubility of mercury based on "like dissolved like". The intermolecular forces between mercury and hydrocarbon molecules are primarily dispersion. For hydrogen force, H-bonding between mercury and hydrocarbon may be considerably low or negligible. The solubility parameters of the studied hydrocarbons are listed in Table 4.7. Toluene and *o*-xylene have additional solubility parameter from polar part. The hydrogen and polar force reduce the dispersion force between mercury and hydrogen molecules. As seen in the case of cyclohexane and aromatics, the solubility of mercury is higher for the former solvent. The results from this work seemed to agree with the experimental data of Spencer and Voigt (1968) at 25°C as presented in Table 4.5. Their mercury solubility in μmole/L was converted to mass fraction (ppb) for comparison purpose, by taking the densities of cyclohexane (d = 0.78 g/cm^3, 25°C), methylcyclohexane (d = 0.769 g/cm^3, 25°C), toluene (d = 0.866 g/cm^3, 25°C) and *o*-xylene (d = 0.881 g/cm^3, 25°C) in the calculation. It was found that the results from this work were lower than that of Spencer and Voigt (1968), but showed similar trend, *i.e.* the solubility in cyclohexane is the highest, comparable between toluene and *o*-xylene, and the lowest in methylcyclohexane.

Table 4.7 Solubility parameters of hydrocarbons at 25°C (Barton, 1991)

Solvent	δ_t	δ_d	δ_p	δ_h
Cyclohexane	16.8	16.8	0.0	0.2
Methylcyclohexane	16.0	16.0	0.0	1.0
Toluene	18.2	18.0	1.4	2.0
o-Xylene	18.0	17.8	1.0	3.1
Ethylbenzene	17.8	17.8	0.6	1.4

δ_t = the total solubility parameter, δ_d = the dispersive component solubility parameter, δ_p = the polar component solubility parameter, δ_h = the hydrogen bonding solubility parameter

The solubility of mercury in ethylbenzene showed abnormal behavior that the mercury solubility at 5°C was extremely high, 17,575 ppb compared to other hydrocarbons or other literature values (Table 4.3). The mercury droplet changed from round and shiny (Figure 4.8, a) to flat and rusty (Figure 4.8, b) appearance. It was noticed that there was formation of fine black particles, the amount increase with time, and the drop shape of mercury became flat. The black particles were suspected to be mercury sulfide and the test of mercuric sulfide was then carried out.

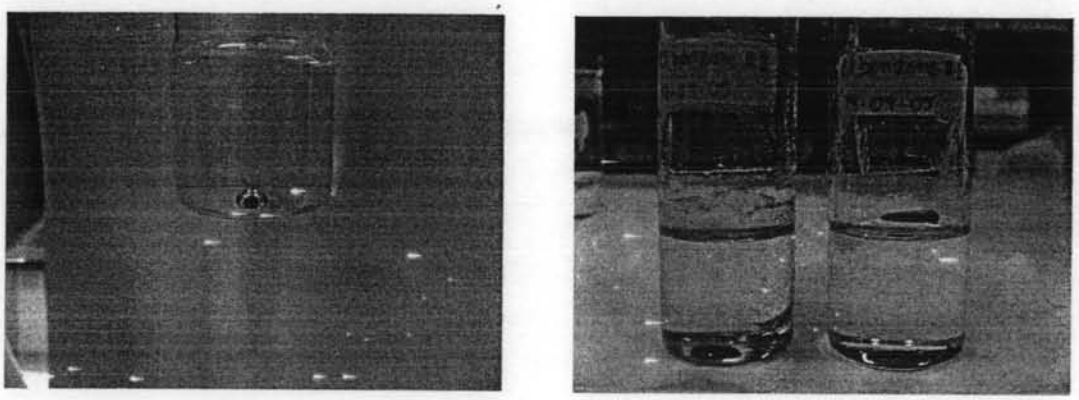

(a) (b)

Figure 4.8 Mercury appearance in (a) other hydrocarbons and (b) ethylbenzene at room temperature.

- Estimation of sulfur content in ethylbenzene.

This test was conducted to ensure whether black particle was mercuric sulfide compound (HgS). The fine black particle sticking on the wall and the bottom of vial was dissolved with nitric acid, digested with bromochloride (BrCl) and analyzed for mercury by cold vapor atomic absorption (CVAAS) followed EPA method 245.7. The mercury concentration of 0.26% was obtained from AAS analysis. Then, the sulfur content was calculated based on the mole equivalent in HgS and it was 0.08 % by weight. The result was estimated, at least 0.08% sulfur content in the ethylbenzene because not the whole black particles, especially the one that sticking on the mercury drop and solubility in the ethylbenzene could not be transferred to AAS analysis. The very high sulfur concentration of 0.08 % would not have been missing in the certification of analysis of ethylbenzene (Appendix E). However, the certification did not state any sulfur content in ethylbenzene. The test of sulfide was further verified.

- Sulfide test (http://wulfenite.fandm.edu/labtech/qualanal.htm)

To confirm the previous result, the sulfide test was performed. Warm 6M hydrochloric acid (HCl) was added to the black particles. If sulfide was presented, it would react with acid to liberate the hydrogen sulfide gas (H_2S) and change a color of a piece of filter paper moistened with lead acetate solution. The test showed no black color of lead acetate (negative result).

- Dissolution of black particle in organic solvents

This experiment was done in order to find other organic solvents that were able to dissolve the black particles. The selected organic solvents were toluene, dichloromethane, ethanol, methanol, and acetone. The selected solvent was added into the vial containing the black particles adsorbing on the mercury mass, and vigorously shaken for 10 minute by hand. The obtained results are shown in Figures 4.9 (a-e). The flat surface of mercury in all solvents became round shape. The mercury appearance in toluene presented one big drop with the shiniest surface while acetone also illustrated a lot of small droplets with the shiny surface. In alcohol solvents (methanol and ethanol), there are a few sizes and a lot of small droplets with dull appearance. The dissolution ability of the black particles was dependent on the polarity of solvents (Table 4.8). Apparently, the black particles dissolved well in the

least polar solvent, *i.e.* toluene and the dissolution decrease with increasing polarity of the solvent. The black particle was possibly organomercury with slight polarity. A lot of small droplets with different sizes of mercury in the solvents were probably due to the different dissolution rate of the black particles. In toluene, the big single drop of mercury was quickly restored because of its fastest rate of dissolution of the black particles, like normal behavior of mercury in other solvents that the big drop of mercury almost instantly forms after stopping the shaking. In acetone, the dissolution rate was the slowest. The remaining of black particles adsorbing on the mercury droplets retarded the agglomeration of droplets.

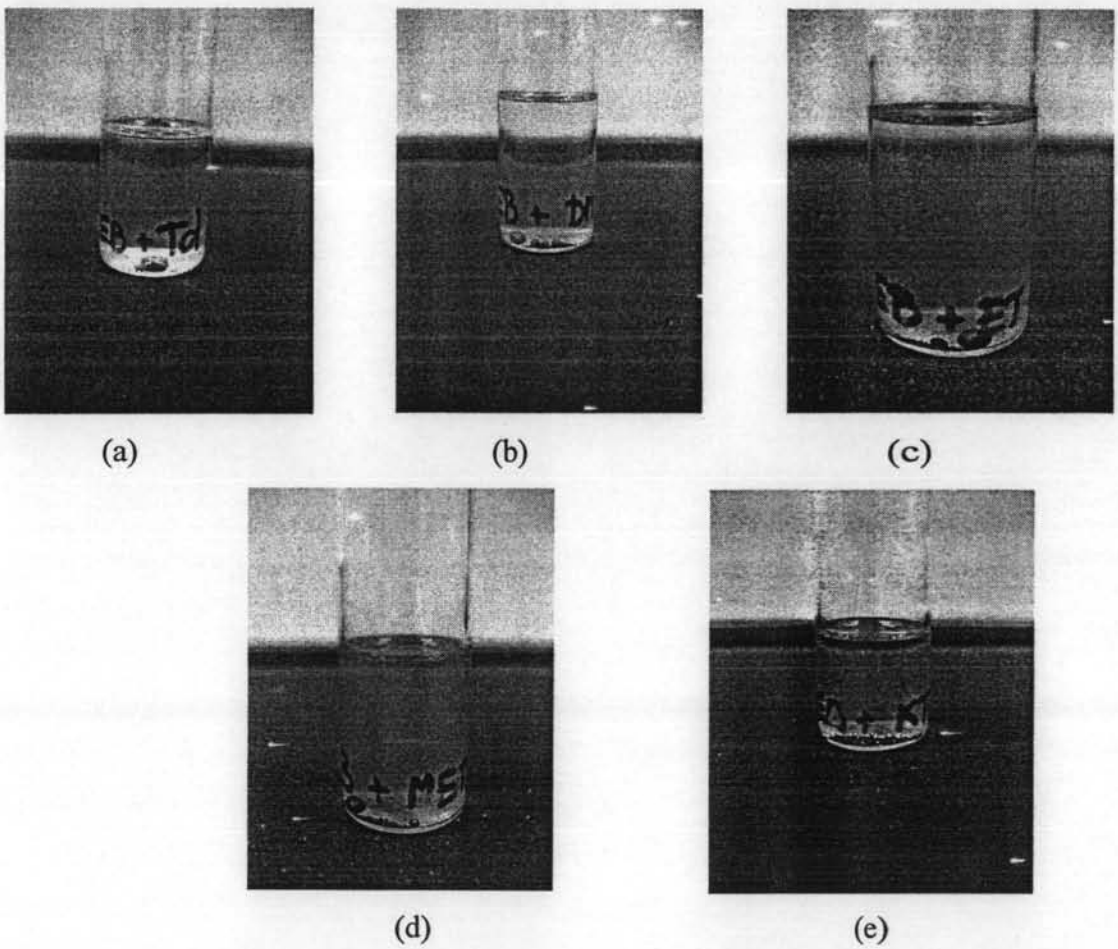

Figure 4.9 Mercury drop appearance in mercury-ethylbenzene system after dissolving in the solvents at room temperature (a) toluene, (b) dichloromethane, (c) ethanol, (d) methanol, (e) acetone.

Table 4.8 Dipole Moment Value of Organic Solvents (John, 1987)

Organic Solvent	Dipole Moment (D)
Toluene	0.45
Dichloromethane	1.60
Ethanol	1.69
Methanol	1.70
Acetone	2.88

- Test of heat stability of black particles

The black particles were tested for heat stability up to 100°C. The black particles and the remaining of mercury mass (Figure 4.10, a) were left in the vial after ethylbenzene was drained off. The vial was gradually heated step by step and the changes were observed and reported in Table 4.9. Figure 4.10 (b) presented mercury drop shape restoring but still dull. In addition, the vial became cloudy and there was the yellow particle residue in the bottom of vial while the black particle diminished. Mercury (II) oxide (HgO) as the yellow particle residue was proposed. Further studies and more detail analysis of these materials are required.

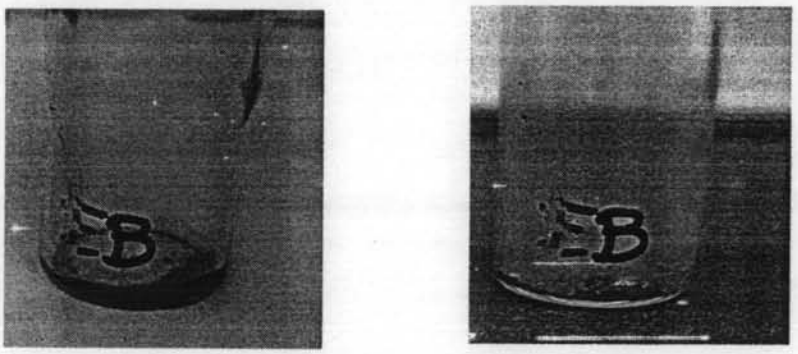

(a) (b)

Figure 4.10 Black particle formation in ethylbenzene system (a) before heating, (b) after heated to 98°C.

Table 4.9 Change in mercury drop from mercury-etylbenzene system during the heating test at temperature range of 28-98°C.

Heating step	Temperature (°C)	Change in mercury drop appearance
1	28	-
2	40	-
3	56	-
4	70	-
5	80	Flat shape, a little shining but still opaque. Fine particles became rust color.
6	90	Flat shape, a little shining but still opaque. Fine particles became rust color.
7	98	Flat shape but rounder than previous step, a little shining but still opaque. Fine particles became rust color.

4.2.2 Solubility of Mercury in Simulated Crude Oil

Apart from single solvent systems, the simulated crude oil made from a mixture of hydrocarbons was also studied. The solubility of mercury in the simulated crude oil shown in Figure 4.11 demonstrated an exponential curve. To compare the solubility of mercury with the single solvent systems, the simulated crude oil curve was plotted together with the single solvent systems as shown in Figure 4.12. The solubility curve of mercury in the simulated crude oil (thick solid line) stayed closer to the solubility curves of those single solvent systems (Rochana, 2006) than those aromatic curves, especially the *n*-decane curve (thick dashed line) at low temperature region (5-25°C) because the composition of simulated crude oil was mainly consisted of *n*-decane (86% by weight). However, the large difference of solubility was observed at high temperature (40°C).

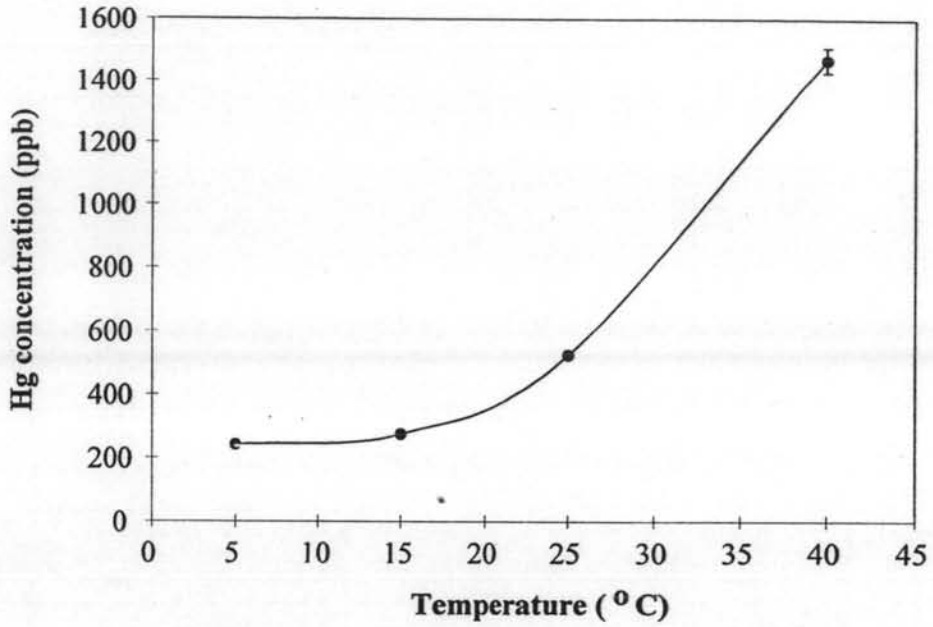

Figure 4.11 Temperature dependence of mercury solubility in the simulated crude oil at the temperature range of 5-40°C.

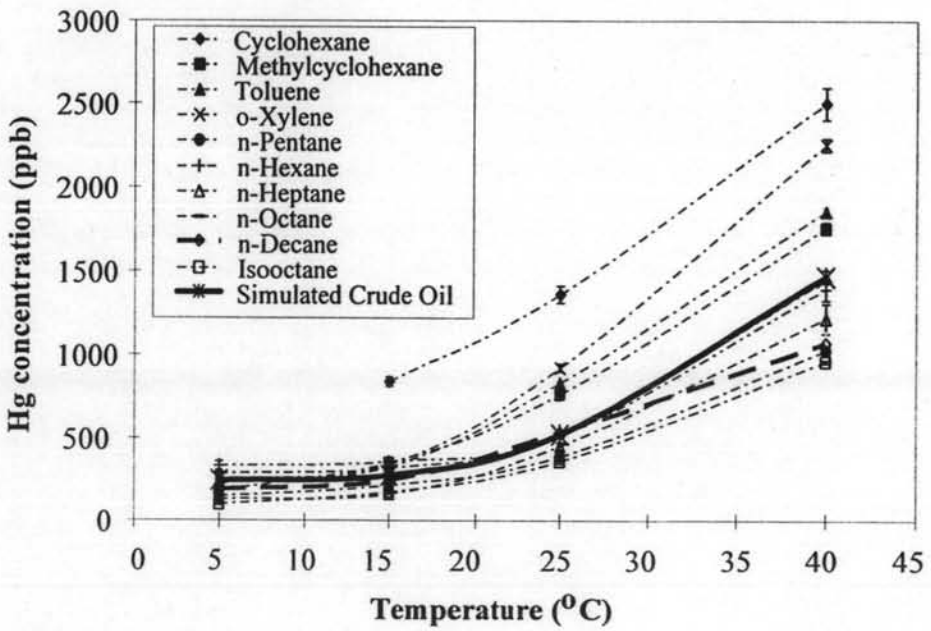

Figure 4.12 Comparison of temperature dependence of mercury solubility in the cyclic aliphatics, aromatics, normal- and branch paraffin (Rochana, 2006) and simulated crude oil at the temperature range of 5-40°C.

The mercury solubility in the simulated crude oil can be calculated or predicted from the summation of mercury solubility multiplied by mole fraction of single solvent.

$$[Hg]_{cal,\ sim\ crude\ oil} = \sum X_i\,[Hg]_{i,exp\ value} \qquad (4.1)$$

Where $[Hg]_{cal,\ sim\ crude\ oil}$ = the calculated mercury solubility in the simulated crude oil

X_i = mole fraction of mercury solubility in single solvent i

$[Hg]_{i,exp\ value}$ = mercury solubility of single solvent i (mole fraction)

The mercury solubility of the calculated crude, the experimental simulated crude, and *n*-decane are tabulated and illustrated in Table 4.10 and Figure 4.13, respectively. There is no calculated result at 5°C owing to the fact that the mercury solubility of cyclohexane cannot be determined. The calculated solubility of the simulated crude oil was very close to the solubility of *n*-decane. The large difference of solubility at high temperature probably came from the synergistic effect of the mixture. Therefore, further studies and more details on binary and ternary system are required.

Table 4.10 Comparison of mercury solubility at increasing temperature

Temperature (°C)	Mole fraction (10^7)		
	The simulated crude oil		*n*-decane
	Experimental value	Calculated value	Experimental value
5	1.60	-	1.33
15	1.81	1.67	1.73
25	3.46	3.58	3.80
40	9.68	7.36	7.60

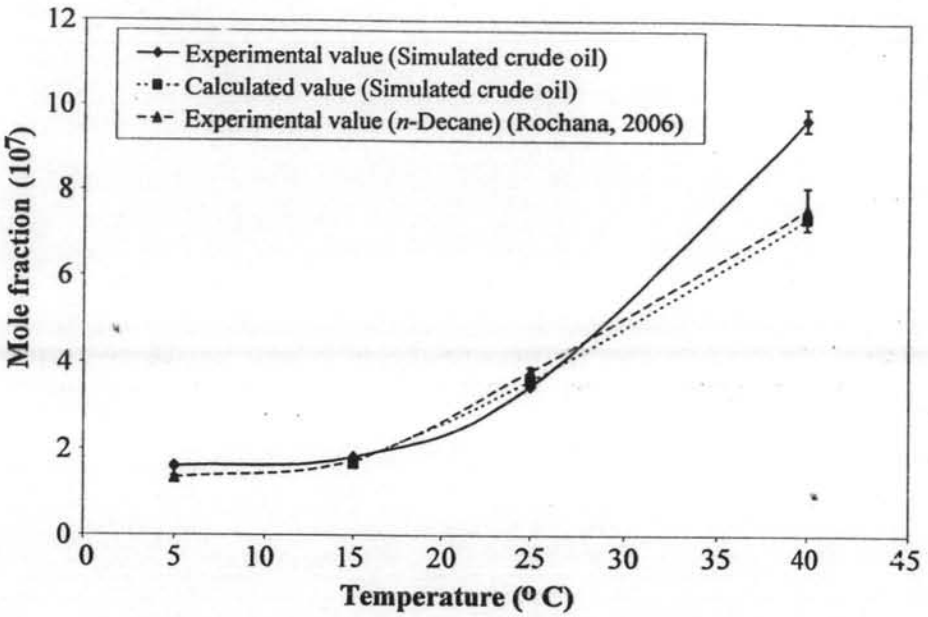

Figure 4.13 Comparison of mercury solubility at increasing temperature at the temperature range of 5-40°C.

4.3 Hysteresis Study

4.3.1 Hysteresis Study in Single Solvent System

The mercury solubility in hydrocarbons was investigated by increasing and then decreasing temperatures. These results are shown in Figures 4.14-4.17, where the solid line and dashed line represent increasing and decreasing temperature, respectively. On decreasing temperature, the differences of mercury solubility at a given temperature in all solvents were in the range of 2 to 220 ppb. The differences of mercury solubility between increasing and decreasing temperature are tabulated in Table 4.11. The interpretation of the solubility differences were carefully done with several assumptions and possibilities shown in Figure 4.18. If the hysteresis existed, pathway I was assumed, *i.e.* kinetics of mercury precipitation, molecular association and organomercury formation. If it did not exist, pathway II was assumed that the difference was insignificant.

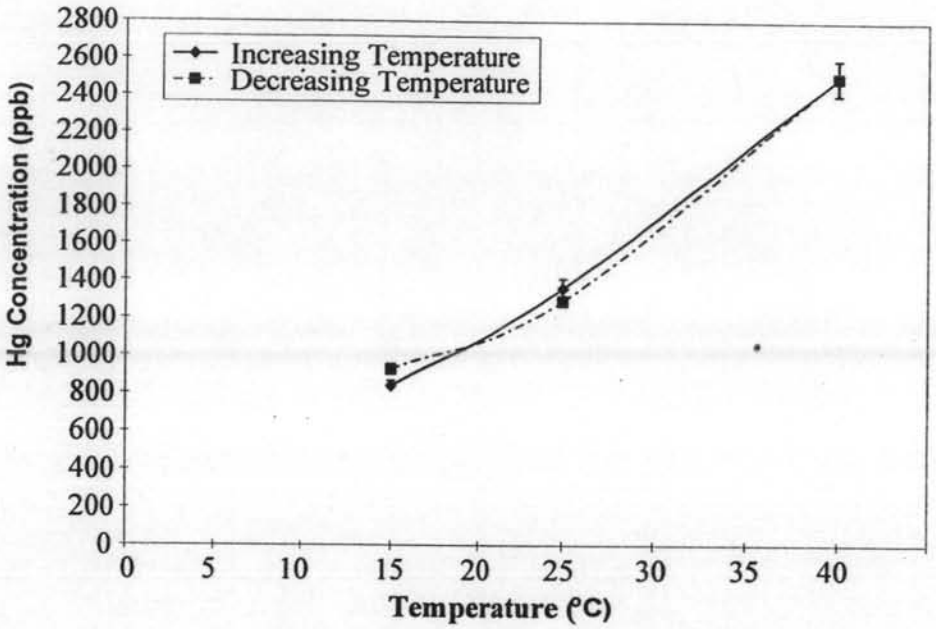

Figure 4.14 Hysteresis study in cyclohexane at the temperature range of 5-40°C.

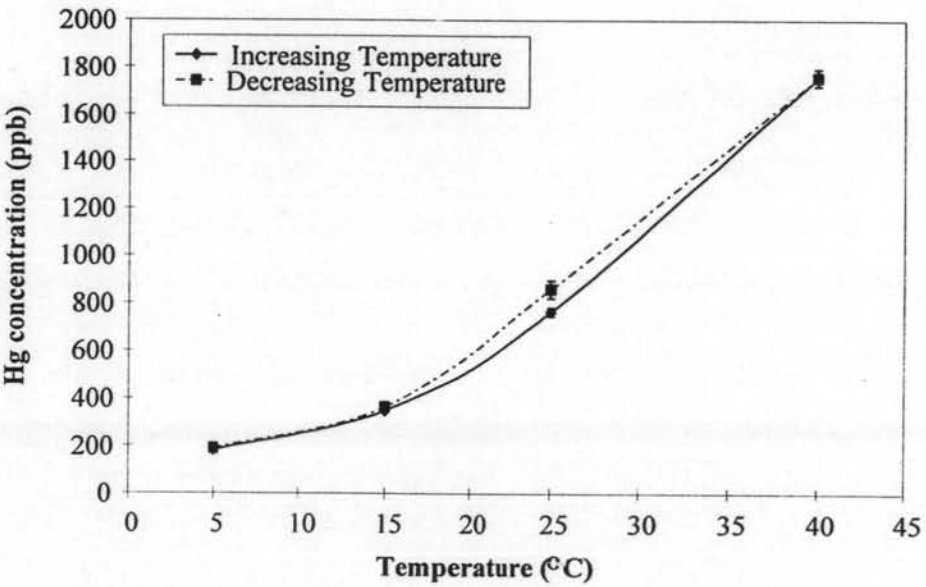

Figure 4.15 Hysteresis study in methylcyclohexane at the temperature range of 5-40°C.

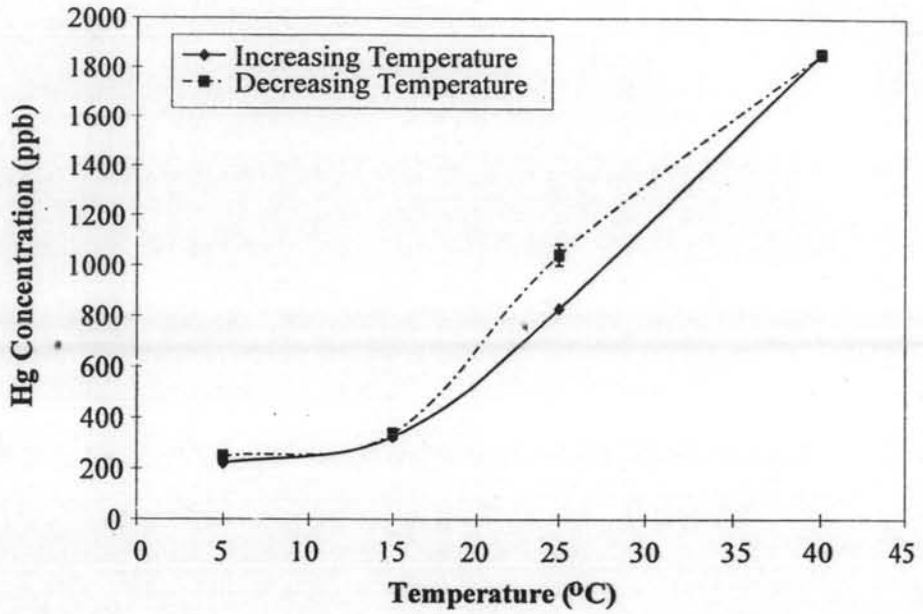

Figure 4.16 Hysteresis study in toluene at the temperature range of 5-40°C.

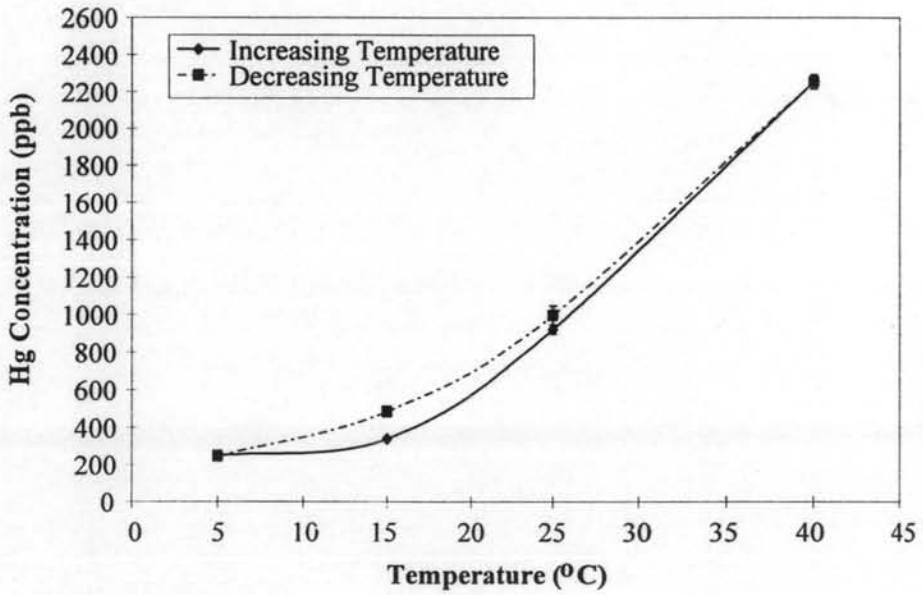

Figure 4.17 Hysteresis study in *o*-xylene at the temperature range of 5-40°C.

Table 4.11 The difference of mercury solubility between decreasing and increasing temperatures

Solvent	Difference (ppb) of solubility at various temperature*		
	5°C	15°C	25°C
Cyclohexane	-	-88	69
Methylcyclohexane	-8	-14	-96
Toluene	-26	-13	-213
o-Xylene	-2	-143	-75

* The solubility at increasing temperature was subtracted from the at decreasing temperature

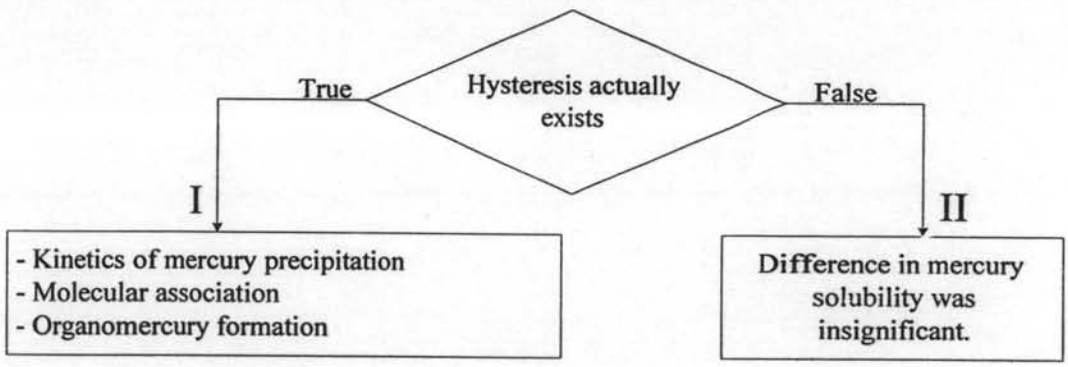

Figure 4.18 Flowchart of possible assumptions for hysteresis study.

1) Kinetics of mercury precipitation

One possibility was due to slow kinetics of mercury precipitation. It was suspected that the solubility of mercury at decreasing temperature might take longer time to reach equilibrium than that of increasing temperature. The equilibration time for hysteresis study was based on the result for the increasing temperature that was performed at 5°C and found that 17 hours was the equilibration time; however, the hysteresis study was set at 20 hours. If this assumption was correct, the mercury concentration on decreasing temperature might take longer time than that of the increasing temperature and the hysteresis would possibly be observed at a lower temperature region. To prove this hypothesis, solubility of mercury at the

decreasing temperature should be monitored for longer period of equilibration and the decreasing temperature curve should overlap the increasing temperature curve.

2) Molecular association

The association of mercury was of interest to a possible explanation on hysteresis. Mercury associating with its own dispersion force tries to reach equilibrium with a drop of mercury from the higher temperature side. The general mechanism of solvation is described in Figure 4.19. The equilibrium should be shifted to the right and reach a new equilibrium concentration. It was proposed that the mercury favors association with hydrocarbon. Thus, the mercury concentration at decreasing temperature would be greater than that at increasing temperature. The decreasing temperature would be located above the increasing temperature line. To prove this assumption, the mercury concentration should be observed for longer period and if hysteresis really existed, the decreasing would still be higher than increasing temperature curve.

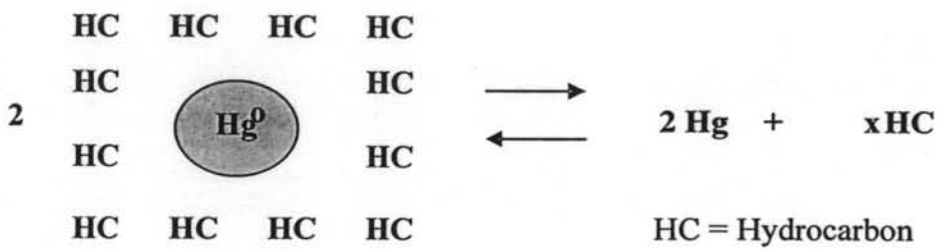

Figure 4.19 The solvation mechanism for mercury in hydrocarbon.

3) Organomercury compounds

The organomercury species could be present and stable in the solvent after the solvent and elemental mercury was equilibrated at the temperature up to 40°C. It was possible as evidently seen in the ethylbenzene system. Then, the dissolved mercury equilibrium (Figure 4.19) would shift to the left side to compensate for the loss. Thus, the hydrocarbon solution would have two mercury species, *i.e.* dissolved elemental mercury and organomercury compound. The solubility of mercury at the decreasing temperature would be higher than at the

increasing temperature and hysteresis would exist. Speciation study of organomercury will be required.

In Figure 4.18, if the assumption agreed with pathway I, the hysteresis curve of such hydrocarbons would be located above the solubility curve of the increasing temperature. On the contrary, in Figure 4.14, the solubility in cyclohexane also showed decreasing temperature line below (at 15°C)and above (at 25°C) the solubility curve of the increasing temperature, but the gap (about 70 ppb) between the curves at 25°C was not seemed to be different (Figure 4.14).

It was suspected that if the difference of mercury solubility between the increasing and decreasing temperatures came from the experimental error, the pathway II was referred to. The actual error in this work was below 5%; however, an acceptable level was the maximum variation at 10% at each temperature (5, 15, and 25°C). New interpretation based on 10% deviation error is shown in Appendix D. The results showed that the hysteresis would not be observed in the cyclohexane and methylcyclohexane systems, but existed in the toluene and *o*-xylene systems (Figures 4.16-17). The results suggested that the solubility parameter of the polar component of aromatics may have a significant effect on the hysteresis.

4.3.2 Hysteresis Study in Simulated Crude Oil

The simulated crude oil was also investigated at decreasing temperature. Figure 4.20 shows the decreasing temperature curve as an s-shape where at low temperature, the curve was on the left and at high temperature, the curve was on the right sides of the increasing temperature curves. The explanation for hysteresis was similar to the proposed explanation for single solvent systems (Figure 4.19). According to Figure 4.20, the gap of mercury solubility between the decreasing and increasing temperature curves was about 30 to 137 ppb. In this case, the hysteresis was clearly observed if it was compared to that of *n*-decane (Rochana, 2006) (86% by weight in the simulated crude oil) as illustrated in Figure 4.21 and the gap difference of solubility was much greater than 10% variation.

The calculated mercury solubility of the simulated crude oil on the decreasing temperature was also compared and presented in Table 4.12 and Figure 4.22. Also, the calculated value of mercury solubility in the simulated crude oil at

decreasing temperature was not able to be determined at 5°C. The calculated results in the simulated crude agreed very well with the experimental result of *n*-decane (Rochana, 2006), but did not agree with the experimental result in the simulated crude oil at 15°C and above. The larger gaps or hysteresis observed in the simulated crude oil were not the effect of addition but possibly due to the synergistic effect of the mixture. Further study in binary and ternary systems will help to clarify this observation.

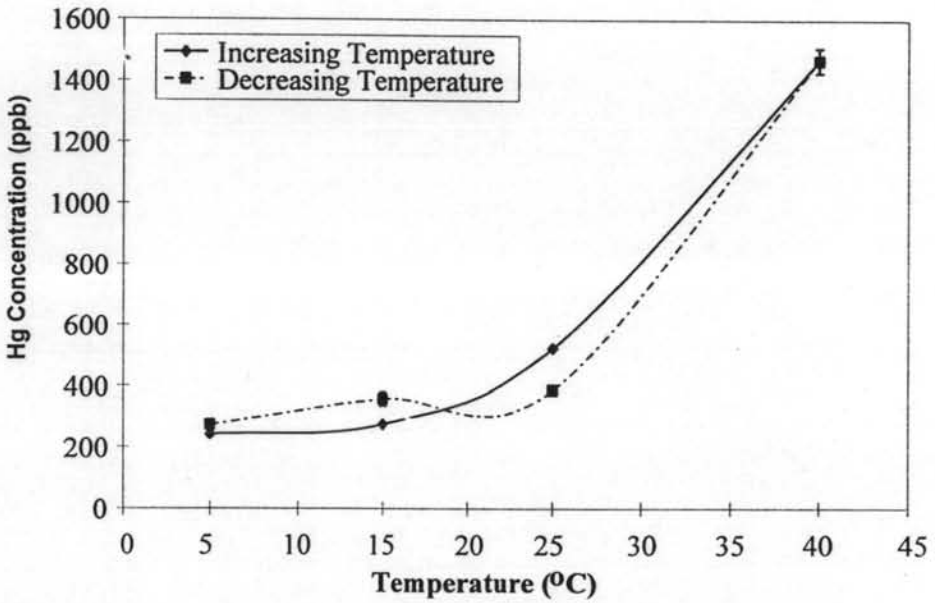

Figure 4.20 Hysteresis study in the simulated crude oil at the temperature range of 5-40°C.

Table 4.12 Comparison of mercury solubility at decreasing temperature

Temperature (°C)	Mole fraction (10^7)		
	The simulated crude oil		*n*-decane
	Experimental value	Calculated value	Experimental value
5	1.80	-	1.37
15	2.36	1.80	1.86
25	2.55	3.57	3.75

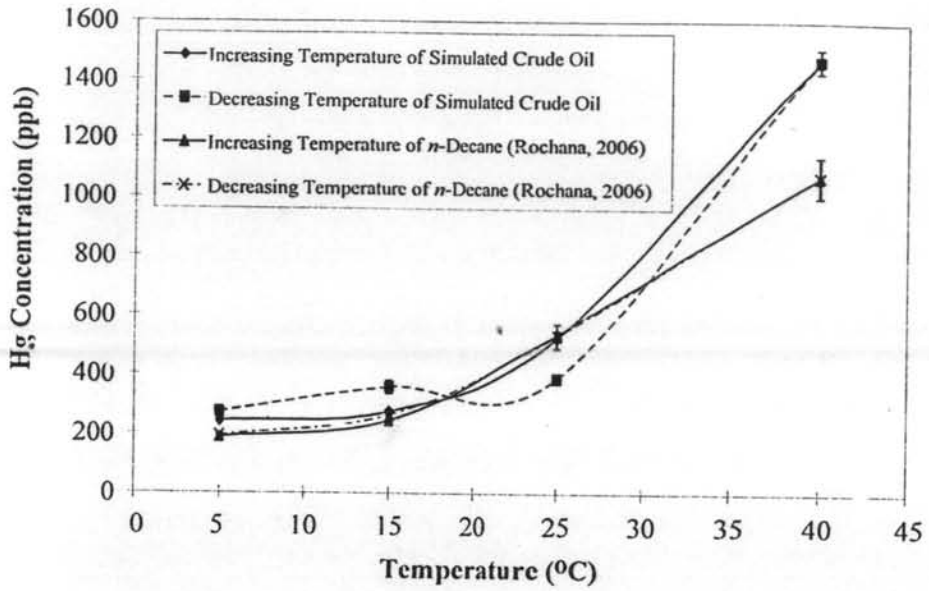

Figure 4.21 Comparison of solubility of mercury between increasing and decreasing temperature at the temperature range of 5-40°C.

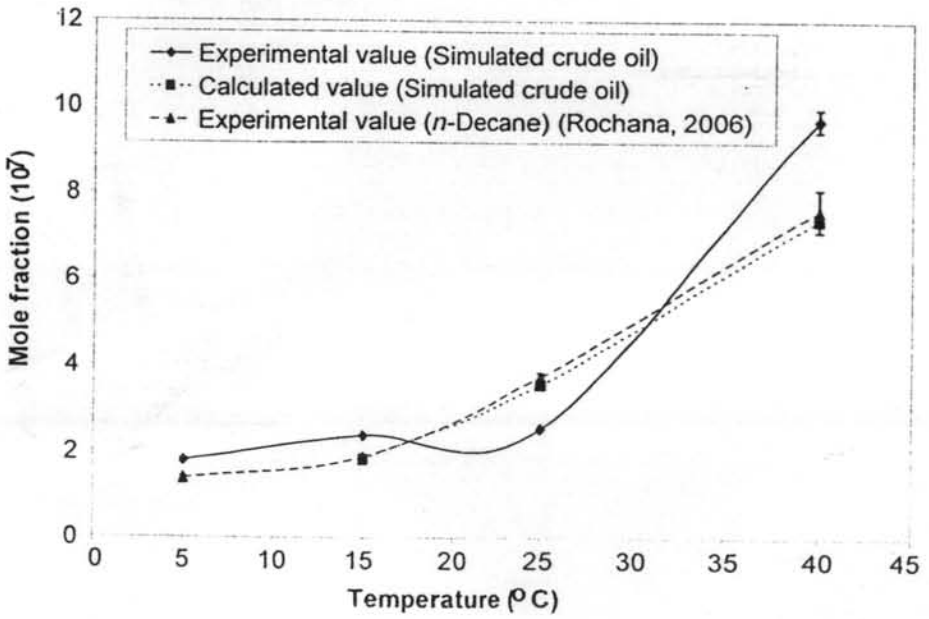

Figure 4.22 Comparison of mercury solubility at decreasing temperature at the temperature range of 5-40°C.